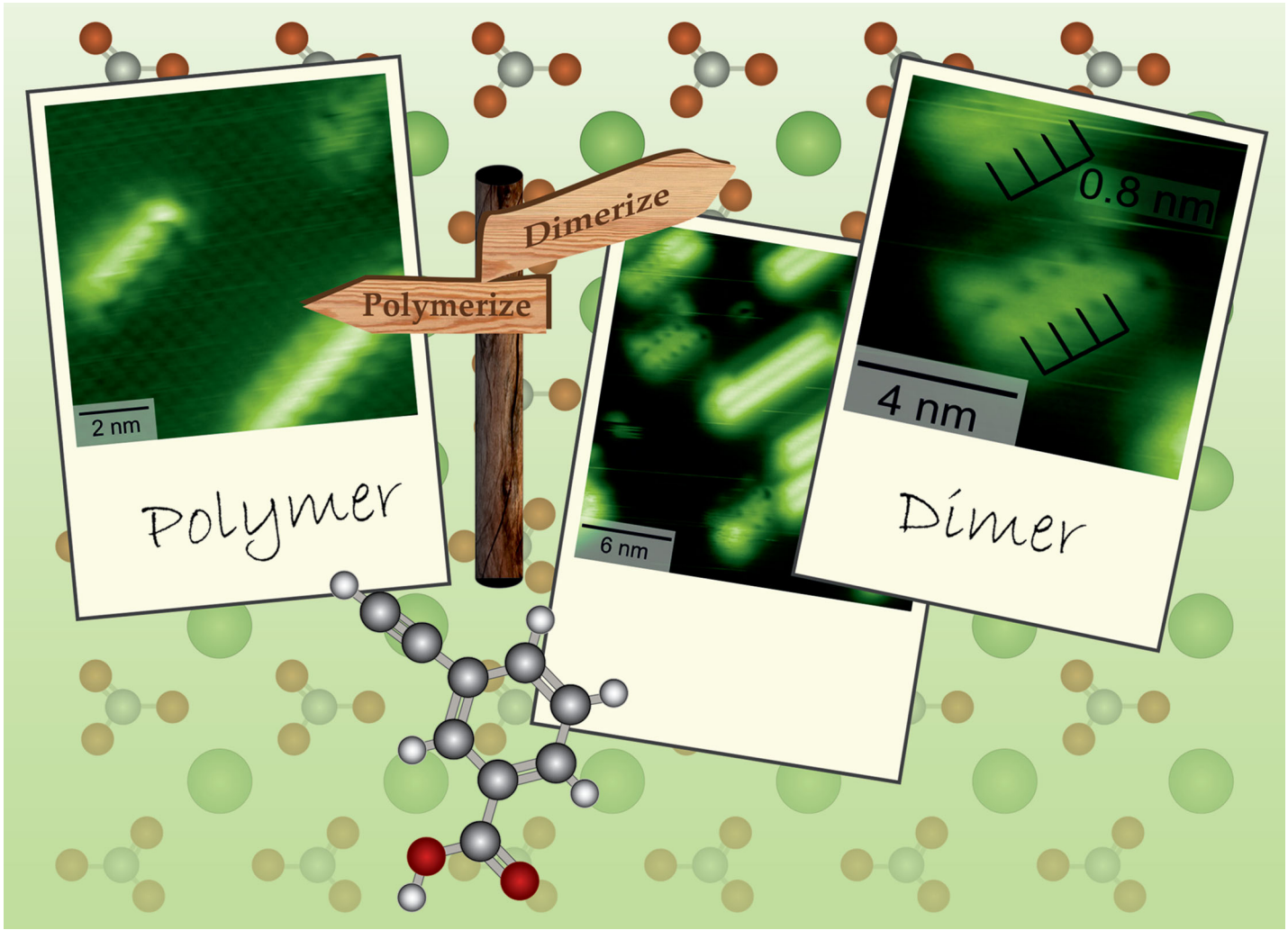

Showcasing research from the group of Professor Angelika Kühnle, Physical Chemistry, Bielefeld University, Germany

Impact of the reaction pathway on the final product in on-surface synthesis

The Kühnle group explores dynamics and structure formation of molecules on surfaces, including molecular self-assembly and on-surface synthesis. An important aspect is elucidating fundamental processes at surfaces and interfaces of dielectric materials. The work in the group comprises method development for advanced imaging both in ultra-high vacuum and at solid–liquid interfaces.

In the current publication, the Kühnle group discloses the impact of surface-controlled reaction pathways on the resulting product in on-surface synthesis. This work highlights the potential of on-surface synthesis for novel reaction control.

As featured in:

See Angelika Kühnle *et al.*, *Phys. Chem. Chem. Phys.*, 2020, **22**, 6109.

ROYAL SOCIETY OF CHEMISTRY

rsc.li/pccp

Registered charity number: 207890

PCCP

PAPER

View Article Online
View Journal | View Issue

Cite this: *Phys. Chem. Chem. Phys.*, 2020, **22**, 6109

Impact of the reaction pathway on the final product in on-surface synthesis†

Antje Kutz,‡[a] Md Taibur Rahman,‡[b] Ville Haapasilta,[c] Chiara Venturini,[d] Ralf Bechstein,[b] André Gordon,[d] Adam S. Foster[ce] and Angelika Kühnle*[b]

Received 6th November 2019,
Accepted 31st January 2020

DOI: 10.1039/c9cp06044h

rsc.li/pccp

On-surface synthesis provides a very promising strategy for creating stable functional structures on surfaces. In the past, classical reactions known from solution synthesis have been successfully transferred onto a surface. Due to the presence of the surface, on-surface synthesis provides the potential of directing the reaction pathway in a manner that might not be accessible in classical solution synthesis. In this work, we present evidence for an acetylene polymerization from a terminal alkyne monomer deposited onto calcite (10.4). Strikingly, although the dimer forms on the surface as well, we find no indication for diacetylene polymerization. This is in sharp contrast to what is observed when directly depositing the dimers on the surface. The different pathways are linked to the specific arrangement of the dimers on the surface. When forming stripes along the [−4−21] direction, the diacetylene polymerization is prohibited, while when arranged in stripes aligned along the [010] direction, the dimers can undergo diacetylene polymerization. Our work thus constitutes a demonstration for controlling the specific reaction pathway in on-surface synthesis by the presence of the surface.

1. Introduction

On-surface synthesis has emerged as a promising approach for the fabrication of functional molecular structures on surfaces.[1–4] Performed in ultrahigh vacuum (UHV), on-surface synthesis provides the option to create products that might not be accessible in classical solution synthesis due to, *e.g.*, the poor solubility[5] or high reactivity of the product.[4] An impressive example for the latter is the synthesis of long acenes,[6] which are unstable under ambient conditions. While nonacene is the largest acene that has been synthesized so far,[7] the synthesis of decacene has been shown by on-surface reduction on a Au(111) surface.[8] In another work, triangulene has been synthesized,[9] a molecule which was predicted in 1953,[10] but never isolated in its unsubstituted form due to its reactivity.

On-surface polymerization[11] of conductive chains is of particular interest for molecular electronics applications as it offers the possibility to create electrical contacts for linking mesoscopic objects with nanoscopic functional units.[12–17] In this context, an elegant example has been presented already in 2001, where the tip of a scanning tunneling microscope has been used to initiate a diacetylene polymerization on a graphite surface.[18,19] However, molecular electronics applications require electrically insulating substrates to decouple the electronic structure of the molecules from the underlying support surface. Recently, we have shown that a diacetylene polymerization can also be induced on the (10.4) surface of calcite, which is a bulk insulator.[20] In the latter study, the dimer formed by homo-coupling of a terminal alkyne has been used as a precursor. Upon deposition onto the surface, the precursors adopt a specific adsorption geometry with a spatially well-defined arrangement. Such geometrical constraints provide the key when aiming for controlling the reaction by surface templating.[21] Given that a specific relative orientation and distance is required for initiating the reaction,[22,23] the arrangement of the precursors on the surface offers a handle for controlling the reaction pathway. Ideally, different reaction pathways should be selectable depending on the specific adsorption configuration. So far, a clear demonstration for reaction selectivity based on surface templating is, however, lacking.

In the present work, we use a terminal alkyne precursor, namely 3-ethynylbenzoic acid (3-EBA, see Fig. 1a), for on-surface synthesis on calcite (10.4) (Fig. 1b). Terminal alkynes are known to undergo Glaser coupling,[24] and the corresponding reaction has

[a] *Institute of Physical Chemistry, Johannes Gutenberg University Mainz, Duesbergweg 10-14, 55099 Mainz, Germany*
[b] *Physical Chemistry I, Faculty of Chemistry, Bielefeld University, Universitätsstraße 25, 33615 Bielefeld, Germany. E-mail: kuehnle@uni-bielefeld.de*
[c] *Department of Applied Physics, Aalto University, PO Box 11100, FI-00076 Aalto, Finland*
[d] *CNRS, CEMES, Nanoscience Group, BP 94347, 29 Rue J. Marvig, 31005 Toulouse, France*
[e] *WPI Nano Life Science Institute (WPI-NanoLSI), Kanazawa University, Kakuma-machi, Kanazawa 920-1192, Japan*

† Electronic supplementary information (ESI) available. See DOI: 10.1039/c9cp06044h

‡ These authors contributed equally to this work.

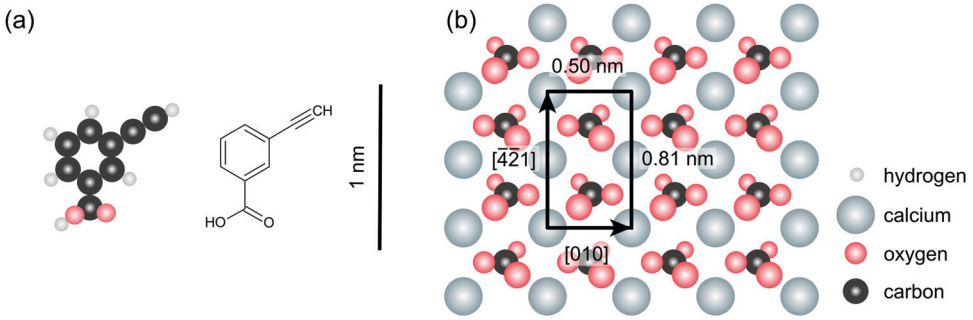

Fig. 1 Model of (a) the 3-ethynylbenzoic acid (3-EBA) molecule and (b) the calcite (10.4) surface. The scale bar applies to both models. The calcite (10.4) surface has a rectangular unit cell with dimensions of (0.50 × 0.81) nm^2, consisting of two carbonate ions and two calcium ions.

been proven to be possible also on metal surfaces.[25–29] We have recently presented the proof of principle that this reaction can also be performed on calcite (10.4).[30] Besides homo-coupling, the precursor used here also has the potential to undergo an acetylene polymerization.[15,31–37] On-surface acetylene polymerization has been shown on Au(111),[37] however, not on a bulk insulator as yet. Here, we provide experimental evidence for on-surface acetylene polymerization using 3-EBA as a precursor. Upon annealing to 550 K, we obtain acetylene polymer chains with lengths of up to 80 nm as deduced from our dynamic atomic force microscopy (AFM) images. Interestingly, although the dimer forms as well, we find no evidence for diacetylene polymerization. This is surprising as diacetylene polymerization is induced when annealing the directly deposited dimer on the surface. The specificity of this reaction pathway can be understood by the different arrangement of the dimers in the two cases: when formed in an on-surface reaction, the dimers form stripes along the [−4−21] direction. When directly deposited, the dimers form stripes along the [010] direction. In these different arrangements, the alignment of the dimers with respect to each other is different, explaining why diacetylene polymerization is possible in one but not the other arrangement.

2. Methods

Experimental part

The calcite crystals used in these experiments were purchased from Korth Kristalle GmbH (Altenholz, Germany). The samples were degassed *in situ* at 700 K for 2 hours prior to cleavage to remove air-borne contaminations. Afterwards, the cleaved crystals were annealed at 650 K for 1 hour to reduce surface charges.

The 3-EBA molecules were purchased from Sigma Aldrich (Germany) or synthesized by us following established procedures.[38–43] Further information on the molecule synthesis can be found in the ESI.† The 3-EBA molecules were sublimated *in situ* from a home-built Knudsen cell. For sublimation, the maximum temperature of the cell was about 310 K. During deposition, the chamber pressure remained below 2×10^{-10} mbar. The molecules were deposited onto a sample kept at room temperature.

All experiments were carried out with a VT AFM 25 atomic force microscope (ScientaOmicron, Taunusstein, Germany) under UHV conditions (base pressure typically better than 4×10^{-11} mbar). All AFM images presented in this work were captured at room temperature. Therefore, all annealed samples were cooled down to room temperature prior to imaging. The system is equipped with an external lock-in amplifier HF2LI (Zurich Instruments AG, Switzerland) to control the phase shift, amplitude and excitation of the oscillation. We used n-doped silicon cantilevers purchased from NanoWorld (Neuchâtel, Switzerland) with an eigen frequency of around 300 kHz (type PPP-NCH). Prior to the measurements, all cantilevers were treated by sputtering with Ar^+ at 2 keV for 10 minutes to remove possible oxide layers as well as other contaminations.

All images shown here are either topography (z_p) or excitation frequency (ν_{exc}) images. The fast and slow scan directions are indicated in the upper right corner in each image. The images are displayed such that under normal imaging conditions (*i.e.*, without contrast inversion[44]) bright colors corresponds to high attractive interactions while dark colors correspond to less attractive or repulsive interactions.

Simulations

All the density functional theory (DFT) computations were performed using the CP2k program suite.[42] We used the PBE functional[43] augmented with the D3 dispersion correction scheme[44] in all computations, both in the structural optimization calculations (T = 0 K) and in the first-principles molecular dynamics (FPMD) simulations. The electronic structure was solved using the Gaussian Plane Wave Method.[45] The valence electrons were expanded in terms of molecularly optimized double-zeta basis functions,[47] whereas the core electronic states were approximated with GTH pseudopotentials.[46] The electronic density was modelled using a plane wave basis with an energy cutoff of 500 Ry. The FPMD simulations were used to explore suitable bonding patterns and to test the stability of the found structures after optimization calculations. The FPMD simulations were run for few thousand steps with a 0.5 fs timestep using velocity rescaling thermostat[45] set to a target temperature of 560 K.

3. Results and discussion

At first, we investigated the adsorption of 3-ethynylbenzoic acid (3-EBA) on calcite (10.4). More specifically, we performed density-functional theory (DFT) calculations to study the binding

geometry of 3-EBA on calcite (10.4). A top and side view of the adsorption geometry is given in Fig. 2a and b, showing a flat-lying molecule. The main axis of the molecule is oriented along the [−4−21] direction with the ring being positioned on a calcium row. The carboxylic acid group binds to the surface *via* a characteristic binding motif:[46] the negatively charged carbonyl oxygen is on top of the positively charged surface calcium, while the hydrogen points to the protruding oxygen atom of the surface carbonate group. The adsorbed molecule exhibits a formation energy of −1.5 eV (with a negative energy being favorable to formation), indicating that the molecule should stick on the surface at room temperature. While this is the most stable configuration we found, there are several other possibilities involving the rotation of the molecule's OH-group within 0.4 eV of the ground state. This flexibility likely explains the high mobility of the monomers on the surface despite the strong adsorption, as at room temperature the molecule will rapidly sample through all these configurations offering paths to translational motion.

To get experimental insights, we sublimated 3-EBA molecules at 310 K for 5 min in front of a freshly cleaved calcite (10.4) surface held at room temperature under UHV conditions and investigated the surface by dynamic AFM at room temperature. In Fig. 2c, a representative AFM image is shown. Two terraces are seen in the image, separated by a step edge. The terraces are decorated by streaky features, which we assign to mobile molecules. No ordered structures are observed at room temperature. From these images, we conclude that the molecules are adsorbed on the calcite (10.4) surface at room temperature, confirming the DFT results presented above. The image indicates that the molecules are highly mobile at room temperature, forming a two-dimensional gas of moving molecules. These are promising conditions for an on-surface reaction.

Next, we present the results of a heating series performed with the sample discussed previously. After heating the molecule-covered sample at 400 K for 1 hour, dot-like bright structures emerged (see Fig. 3a). The streaky features observed on the as-deposited sample were still present, indicative of mobile molecules. When increasing the heating temperature to 450 K for 1 hour, the streaky features nearly vanished. Most importantly, stripe-like structures were formed along the [−4−21] direction (see Fig. 3b). Upon heating at 550 K for 1 hour, these stripe-liked structures appeared longer in length (more than 20 nm in Fig. 3c). We could increase the stripe length up to 80 nm upon dosing more monomers and annealing for longer times (see ESI,† Fig. S1). The streaky features have completely vanished and only few dot-like clusters remained after heating at 550 K.

To investigate the inner structure of the emerging stripes, we performed high-resolution imaging of a stripe-covered area. As can be seen in Fig. 4a, two different stripe-like structures exist, which are both aligned along the [−4−21] direction. As will be argued in the following, these two structures are assigned to (1) polyacetylene chains and (2) side-by-side aligned dimers.

The majority of the stripes (marked by the red box in Fig. 4) show a periodicity of 0.4 nm along the [−4−21] direction, corresponding to the calcium–calcium distance in this direction (see Fig. 4b and c). Terminal alkynes are known to react *via* an acetylene polymerization.[31] To investigate whether the stripes formed here indeed constitute acetylene polymers, we again performed DFT calculations. We compared the formation energy of the polymer on the surface with the equivalent number of monomers, *i.e.*, isolated 3-EBA molecules, maintaining compatible atom numbers in both energy evaluations. We found that the acetylene polymer chain has a formation energy, which is 1.1 eV per molecule lower than the energy of isolated 3-EBA molecules on calcite (10.4). This calculation suggests that an acetylene polymer on the surface should be more favorable than the unreacted monomers. Moreover, the calculated *cis–transoidal* polymer structure fits excellently to the observed stripe structure, as demonstrated in Fig. 4d. With these results, we conclude that an acetylene polymerization can be achieved *via* the deposition of the monomer precursor, 3-EBA, onto calcite (10.4).[47]

In principle, the 3-EBA monomer used here also has the possibility to undergo dimerization.[25] When depositing this dimer directly onto calcite (10.4), we have previously shown that it undergoes diacetylene polymerization.[20] This leads to the interesting question as to why there is no indication of diacetylene polymerization upon deposition of the 3-EBA monomer. Does no dimer form? For this, we return to the second structure formed, which is marked by the blue box in Fig. 4a.

In these stripes, dark dots at the periphery of the stripes are observed, which exhibit a periodicity of 0.8 nm along the [−4−21] direction, which corresponds to the unit cell dimension

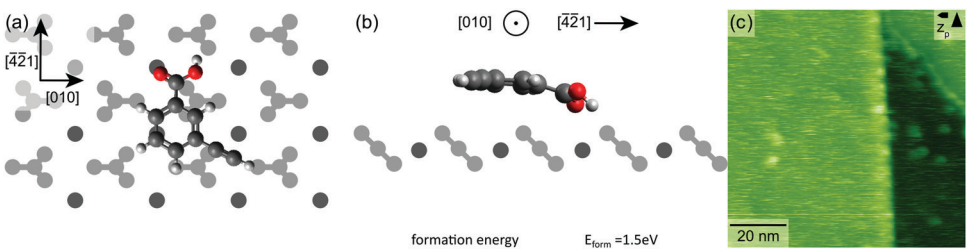

Fig. 2 Optimized geometry of an isolated 3-EBA molecule on the calcite (10.4) surface in (a) top view and (b) side view. (c) AFM topography image of an as-deposited calcite (10.4) sample. Two step edges are seen in the image. The terraces are covered by streaky features, indicating mobile species on the surface at room temperature.

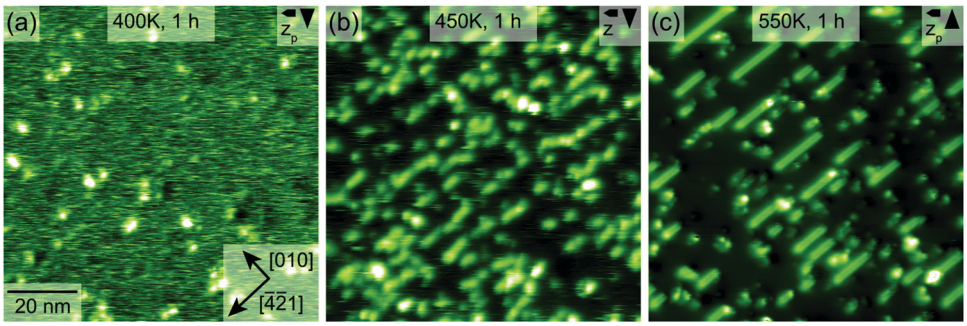

Fig. 3 Examples from a heating series of a molecule-covered sample. Each annealing step lasted for 1 hour. (a) Heating to 400 K led to the formation of some bright dots, while (b) heating to 450 K resulted in a reduction of the streaky features and the appearance of stripe-like structures, oriented in the [−4−21] direction. Further heating to (c) 550 K yielded in longer stripes and the disappearance of the streaky features.

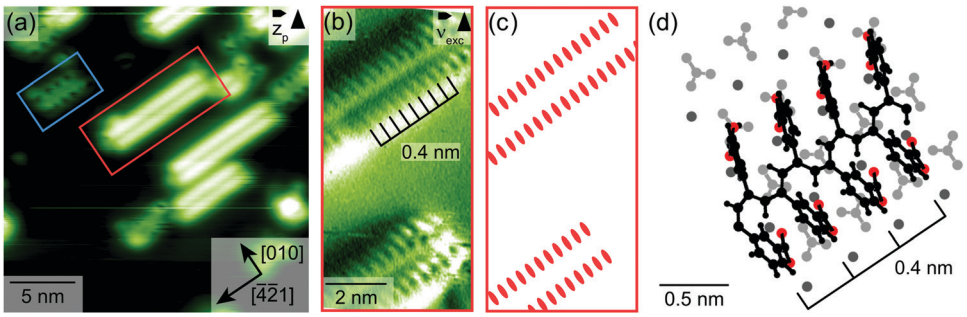

Fig. 4 Molecular structure obtained upon heating the sample for 1 h to 550 K. (a) Two different kind of stripes can be seen along the [−4−21] direction, marked by red and blue boxes, respectively. (b) The stripe marked by the red box in (a) is shown in a frequency shift image, revealing the periodicity of 0.4 nm. (c) Sketch illustrating the inner structure of the stripes. (d) Acetylene polymer structure as obtained from DFT, including the calcite (10.4) surface to illustrate the excellent match in size and pattern.

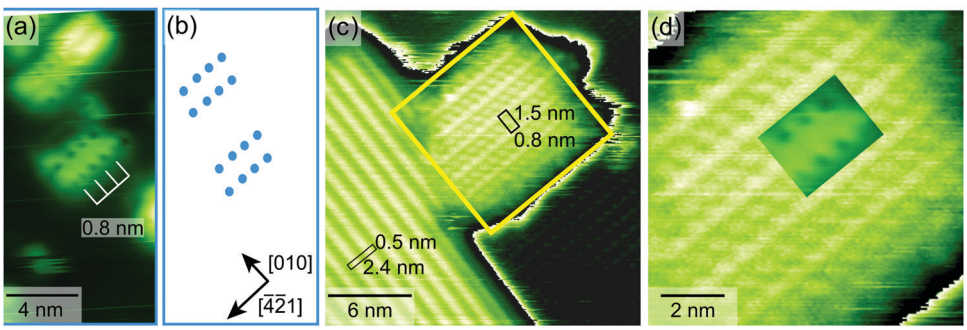

Fig. 5 (a) Zoom-in AFM image of second structure formed upon heating the 3-EBA monomer deposited on calcite (10.4) surface, exhibiting the periodicity of 0.8 nm. (b) Sketch illustrating the inner structure of the stripes. (c) Structure observed after direct deposition of the dimer. The yellow box highlights an island composed of stripes oriented along the [−4−21] direction. (d) An area from (a) is superimposed onto the island shown in image (c).

in this direction (see Fig. 5(a and b)). To obtain further insights into this structure, we compare these stripes with the previously reported arrangement of the dimer molecules when directly deposited onto calcite (10.4).[20] When directly deposited onto calcite (10.4), the dimers form islands composed of rows running along the [010] direction. However, a second island structure is found that was reported in our previous work,[20] composed of rows oriented along the [−4−21] direction (see Fig. 5c). These rows exhibit a periodicity of 0.8 nm along the row direction and do, indeed, resemble the second stripes observed here. When an image of the second stripe structure is superimposed onto the island, the excellent fit in dimensions becomes evident (see Fig. 5d), indicating that the second stripe structure found here is composed of side-by-side arranged dimers resulting in rows oriented in the [−4−21] direction.

In summary, the two different reaction products observed here are assigned to (1) polyacetylene chains and (2) side-by-side aligned dimers. The latter finding is surprising because it shows that the monomer indeed undergoes homo-coupling and forms dimers, however, no further reaction towards diacetylene polymers is observed (see Fig. 6). This result demonstrates that a different pathway is taken when the monomer is

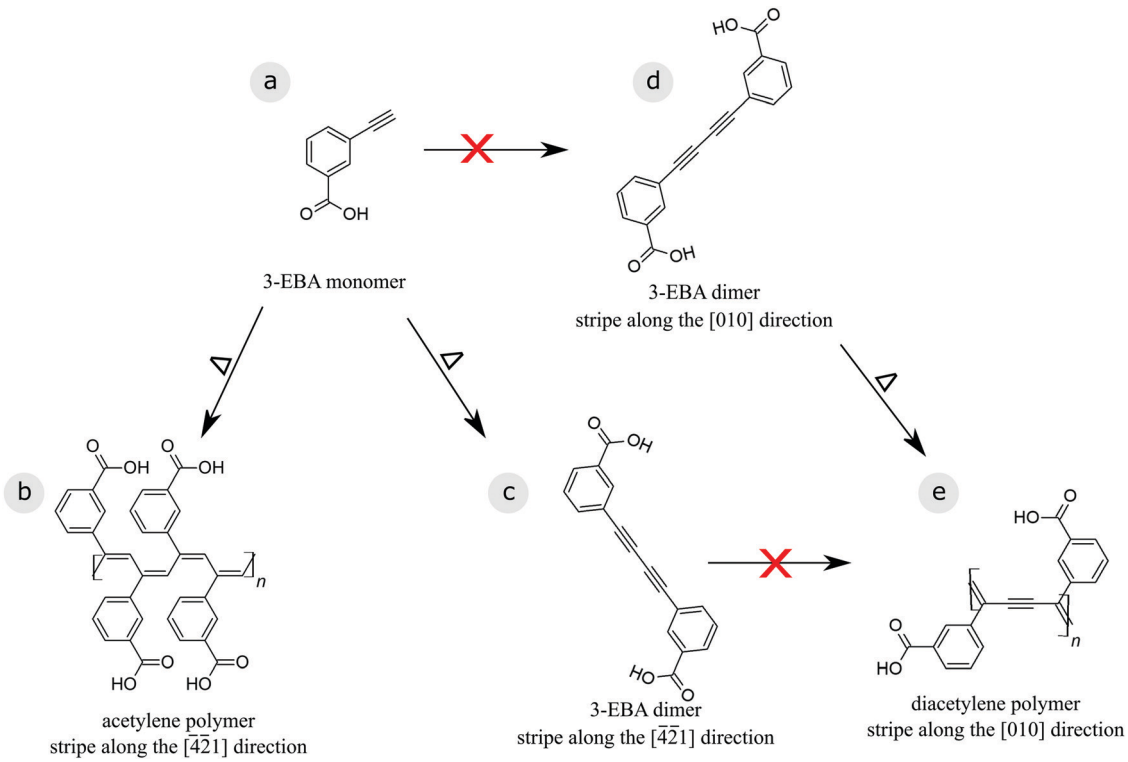

Fig. 6 Overview of the reaction pathways of the 3-EBA monomer (a) on calcite (10.4). Upon annealing, acetylene polymerization can be induced (b). The monomer can also form homo-coupled dimers. These dimers align side-by-side and form rows along the [−4−21] direction (c). Interestingly, in this arrangement, the dimers do not react further. When directly depositing the dimers, rows arranged in the [010] direction form (d). Only in this arrangement, the dimers undergo diacetylene polymerization (e).

deposited and only forms dimers on the surface as compared to depositing the dimer directly. In both cases, dimers are present on the surface and arrange side-by-side to form stripes, however, when depositing the dimers directly, the stripes are predominantly aligned along the [010] direction with a periodicity of 0.5 nm along the stripe.[20] In this arrangement, the dimer spacing is in the reported range required for diacetylene polymerization of 0.47 to 0.52 nm and also the angle of the molecular axis with respect to stripe matches the angle of 45°, which has been mentioned in literature.[23] In contrast to the situation observed after depositing the dimers directly, when the dimers are only formed on the surface, the stripes are aligned along the [−4−21] direction. Here, the periodicity along the stripe is 0.8 nm, which is significantly larger than what has been reported for diacetylene polymerization.[23] In this case, the dimers do not further react to diacetylene polymers. This comparison demonstrates that, even that the same molecule is present on the surface in both cases, the specific reaction conditions governs the reaction pathway that is taken.

4. Conclusion

In conclusion, by the interplay of dynamic AFM experiments and DFT computations we present evidence for an acetylene polymerization carried out on a bulk insulator surface. The terminal alkyne precursor molecule, 3-EBA, used in this work forms a two-dimensional gas of mobile molecules on the surface when deposited at room temperature on calcite (10.4). Heating the sample at 550 K results in the formation of stripes along the [−4−21] direction, which match excellently match with *cis–trans-oidal* acetylene polymer chains. This assignment is further corroborated by the DFT calculations, revealing that the acetylene polymerization is associated with an energy gain of 1.1 eV per acetylene unit formed. Moreover, another type of stripe oriented along the [−4−21] direction can be found that is identical to a structure formed upon direct deposition of the dimer. Therefore, we assign these stripes to an arrangement of side-by-side aligned dimers.

Most interestingly, we find no evidence for a further reaction of the latter dimers to form a diacetylene polymer. This is in sharp contrast to what has been found previously when directly depositing the dimers. Thus, our result demonstrates that the constraint given by the specific reaction pathway can effectively control the final product: when the dimer is deposited directly, the diacetylene polymerization is induced. In sharp contrast, when the dimer is only formed in an on-surface reaction from the monomer precursor, the diacetylene polymerization is effectively prohibited. Our work provides a clear example of how the specific reaction pathway in on-surface synthesis affects the final product.

Conflicts of interest

The authors declare no conflicts of interest.

Acknowledgements

We gratefully acknowledge financial support from the EU through grant PAMS (seventh framework program GA 610446). Computing resources from the Aalto Science-IT project and CSC IT Center for Science, Finland, are gratefully acknowledged. This work was furthermore supported by the Academy of Finland through its Centres of Excellence Programme 2015–2017 under project number 284621, as well as project 314877. A. S. F. was supported by the World Premier International Research Center Initiative (WPI), MEXT, Japan.

References

1 A. Gourdon, *Angew. Chem., Int. Ed.*, 2008, **47**, 6950–6953.
2 R. Lindner and A. Kühnle, *ChemPhysChem*, 2015, **16**, 1582–1592.
3 A. Richter, A. Floris, R. Bechstein, L. Kantorovich and A. Kühnle, *J. Phys.: Condens. Matter*, 2018, **30**, 133001.
4 G. Franc and A. Gourdon, *Phys. Chem. Chem. Phys.*, 2011, **13**, 14283–14292.
5 M. Treier, C. A. Pignedoli, T. Laino, R. Rieger, K. Müllen, D. Passerone and R. Fasel, *Nat. Chem.*, 2011, **3**, 61–67.
6 J. I. Urgel, H. Hayashi, M. Di Giovannantonio, C. A. Pignedoli, S. Mishra, O. Deniz, M. Yamashita, T. Dienel, P. Ruffieux, H. Yamada and R. Fasel, *J. Am. Chem. Soc.*, 2017, **139**, 11658–11661.
7 C. Tönshoff and H. F. Bettinger, *Angew. Chem., Int. Ed.*, 2010, **49**, 4125–4128.
8 J. Krüger, F. García, F. Eisenhut, D. Skidin, J. M. Alonso, E. Guitián, D. Pérez, G. Cuniberti, F. Moresco and D. Peña, *Angew. Chem., Int. Ed.*, 2017, **56**, 11945–11948.
9 N. Pavliček, A. Mistry, Z. Majzik, N. Moll, G. Meyer, D. J. Fox and L. Gross, *Nat. Nanotechnol.*, 2017, **12**, 308–311.
10 E. Clar and D. G. Stewart, *J. Am. Chem. Soc.*, 1953, **75**, 2667–2672.
11 F. Para, F. Bocquet, L. Nony, C. Loppacher, M. Féron, F. Cherioux, D. Z. Gao, F. Federici Canova and M. B. Watkins, *Nat. Chem.*, 2018, **10**, 1112–1117.
12 A. J. Heeger, *Angew. Chem., Int. Ed.*, 2001, **40**, 2591–2611.
13 H. Shirakawa, *Angew. Chem., Int. Ed.*, 2001, **40**, 2574–2580.
14 A. G. MacDiarmid, *Angew. Chem., Int. Ed.*, 2001, **40**, 2581–2590.
15 D. J. Sandman, J. M. Njus and B. Tran, *Macromol. Symp.*, 2004, **216**, 77–85.
16 C. X. Wang, J. L. Chen, C. H. Shu, K. J. Shi and P. N. Liu, *Phys. Chem. Chem. Phys.*, 2019, **21**, 13222–13229.
17 J. Y. Dai, Q. T. Fan, T. Wang, J. Kuttner, G. Hilt, J. M. Gottfried and J. F. Zhu, *Phys. Chem. Chem. Phys.*, 2016, **18**, 20627–20634.
18 Y. Okawa and M. Aono, *Nature*, 2001, **409**, 683–684.
19 Y. Okawa and M. Aono, *J. Chem. Phys.*, 2001, **115**, 2317–2322.
20 A. Richter, V. Haapasilta, C. Venturini, R. Bechstein, A. Gourdon, A. S. Foster and A. Kühnle, *Phys. Chem. Chem. Phys.*, 2017, **19**, 15172–15176.
21 R. Lindner, P. Rahe, M. Kittelmann, A. Gourdon, R. Bechstein and A. Kühnle, *Angew. Chem., Int. Ed.*, 2014, **53**, 7952–7955.
22 G. Wegner, *Pure Appl. Chem.*, 1977, **49**, 443–454.
23 K. Fahsi, J. Deschamps, K. Chougrani, L. Viau, B. Boury, A. Vioux, A. van der Lee and S. G. Dutremez, *CrystEngComm*, 2013, **15**, 4261–4279.
24 C. Glaser, *Ber. Dtsch. Chem. Ges.*, 1869, **2**, 422–424.
25 F. Klappenberger, Y.-Q. Zhang, J. Björk, S. Klyatskaya, M. Ruben and J. V. Barth, *Acc. Chem. Res.*, 2015, **48**, 2140–2150.
26 H.-Y. Y. Gao, J.-H. H. Franke, H. Wagner, D. Zhong, P.-A. A. Held, A. Studer and H. Fuchs, *J. Phys. Chem. C*, 2013, **117**, 18595–18602.
27 H.-Y. Y. Gao, H. Wagner, D. Zhong, J.-H. Franke, A. Studer and H. Fuchs, *Angew. Chem., Int. Ed.*, 2013, **52**, 4024–4028.
28 H.-Y. Y. Gao, D. Zhong, H. Mönig, H. Wagner, P.-A. Held, A. Timmer, A. Studer and H. Fuchs, *J. Phys. Chem. C*, 2014, **118**, 6272–6277.
29 J. Liu, Q. W. Chen, Q. L. He, Y. J. Zhang, X. Y. Fu, Y. F. Wang, D. H. Zhao, W. Chen, G. Q. Xu and K. Wu, *Phys. Chem. Chem. Phys.*, 2018, **20**, 11081–11088.
30 A. Richter, M. Vilas-Varela, D. Peña, R. Bechstein and A. Kühnle, *Surf. Sci.*, 2018, **678**, 106–111.
31 S. J. Landon, P. M. Shulman and G. L. Geoffroy, *J. Am. Chem. Soc.*, 1985, **107**, 6739–6740.
32 T. J. Katz and S. J. Lee, *J. Am. Chem. Soc.*, 1980, **102**, 422–424.
33 T. J. Katz, S. J. Lee and M. A. Shippey, *J. Mol. Catal.*, 1980, **8**, 219–226.
34 K. Judai, S. Abbet, A. S. Worz, A. M. Ferrari, L. Giordano, G. Pacchioni and U. Heiz, *J. Mol. Catal. A: Chem.*, 2003, **199**, 103–113.
35 T. Masuda, Y. Kuwane, K. Yamamoto and T. Higashimura, *Polym. Bull.*, 1980, **2**, 823–827.
36 G. Natta and F. Danusso, *Stereoregular Polymers and Stereospecific Polymerizations*, Pergamon, Elsevier, 1967.
37 A. Riss, S. Wickenburg, P. Gorman, L. Z. Tan, H. Z. Tsai, D. G. de Oteyza, Y. C. Chen, A. J. Bradley, M. M. Ugeda, G. Etkin, S. G. Louie, F. R. Fischer and M. F. Crommie, *Nano Lett.*, 2014, **14**, 2251–2255.
38 D. A. Offermann, J. E. McKendrick, J. J. P. Sejberg, B. L. Mo, M. D. Holdom, B. A. Helm, R. J. Leatherbarrow, A. J. Beavil, B. J. Sutton and A. C. Spivey, *J. Org. Chem.*, 2012, 77, 3197–3214.
39 E. Merkul, D. Urselmann and T. J. J. Müller, *Eur. J. Org. Chem.*, 2011, 238–242.
40 W. B. Austin, N. Bilow, W. J. Kelleghan and K. S. Y. Lau, *J. Org. Chem.*, 1981, **46**, 2280–2286.
41 Y. S. Feng, C. Q. Xie, W. L. Qiao and H. J. Xu, *Org. Lett.*, 2013, **15**, 936–939.
42 L. F. Jones, M. E. Cochrane, B. D. Koivisto, D. A. Leigh, S. P. Perlepes, W. Wernsdorfer and E. K. Brechin, *Inorg. Chim. Acta*, 2008, **361**, 3420–3426.
43 R. H. Pawle, V. Eastman and S. W. Thomas, *J. Mater. Chem.*, 2011, **21**, 14041–14047.
44 F. Loske, P. Rahe and A. Kühnle, *Nanotechnology*, 2009, **20**, 264010.
45 G. Bussi, D. Donadio and M. Parrinello, *J. Chem. Phys.*, 2007, **126**, 014101.
46 D. M. Duffy and J. H. Harding, *Langmuir*, 2004, **20**, 7630–7636.
47 See the ESI† for a detailed discussion of other reasonable reaction pathways, in which we provide arguments for discarding all other obvious reaction products.

